

Research Article

## Virtual screening and molecular dynamics simulation studies to predict the binding of *Sisymbrium irio* L. derived phytochemicals against *Staphylococcus aureus* dihydrofolate reductase (DHFR)

### Madhurima Tiwari

Institute of Biosciences and Technology, Shri Ramswaroop Memorial University, Village Hadauri, Post- Tindola, Lucknow-Deva Road, Barabanki (Uttar Pradesh), India

### Sunita Gupta

Department of Biotechnology, Jaypee Institute of Information Technology, Noida (Uttar Pradesh), India

### Prachi Bhargava\*

Institute of Agricultural Sciences and Technology, Shri Ramswaroop Memorial University, Village Hadauri, Post- Tindola, Lucknow-Deva Road, Barabanki (Uttar Pradesh), India

\*Corresponding author. Email: prachibhargava51@gmail.com

### Article Info

<https://doi.org/10.31018/jans.v14i4.3641>

Received: July 7, 2022

Revised: November 8, 2022

Accepted: November 16, 2022

### How to Cite

Tiwari, M. *et al.* (2022). Virtual screening and molecular dynamics simulation studies to predict the binding of *Sisymbrium irio* L. derived phytochemicals against *Staphylococcus aureus* dihydrofolate reductase (DHFR). *Journal of Applied and Natural Science*, 14(4), 1297 - 1307. <https://doi.org/10.31018/jans.v14i4.3641>

### Abstract

The discovery of antibiotics initiated the era of drug innovation and implementation for human and animal health. Very soon, antibiotic resistance started evolving due to over-prescription and heavy usage of drugs leading to deleterious side effects. However, using plant extracts or medicinal plants has emerged as a new approach to dealing with the current problem. One such medicinal plant *Sisymbrium irio* L. is widely used in Unani therapy as an antimicrobial, analgesic, antipyretic, antioxidant, anti-inflammatory, hepatoprotective, bronchoprotective etc. The phytochemicals extracted from the aerial part of the plant have been used as a natural compound library and screened against a well-known anti-bacterial drug target Dihydrofolate reductase (DHFR) enzyme of *Staphylococcus aureus*. The top two phytochemicals with lower docking score along with the positive control were subjected to molecular dynamics (MD) simulation studies to examine the stabilities of the complexes over 100 ns, followed by binding free energy estimation. The Root Mean Square Deviation (RMSD), Root Mean Square Fluctuation (RMSF) and Radius of Gyration (Rg) yielded established results throughout the MD run. Moreover, the derived phytochemicals exhibited lower binding free energy values than the positive control that can be tested for its *in vitro* efficacy, followed by further optimization to attain a potent therapeutic against *S. aureus*. Taken together, the present study suggests two promising phytochemicals derived from the aerial part of the plant *S. irio* with stable MD simulation results, strong binding affinity and no side effects.

**Keywords:** Binding free energy, DHFR, Phytochemicals, *Sisymbrium irio* L.

### INTRODUCTION

In recent years, commercially used antibiotics have decreased in their actions due to the emergence of resistance in pathogenic bacteria (Adwan *et al.*, 2010). Therefore, the researchers focus on the plants and their phyto-constituents having antimicrobial properties (Al Akeel *et al.*, 2014). These phytochemicals may act on DNA replication, protein synthesis and cell wall synthesis during the division cycle of the bacterial cell (Alves *et al.*, 2014). One of the medicinal plants *Sisymbrium*

*irio* L. commonly known as London Rocket of the family 'Brassicaceae' is distributed in different parts of the world (Khoshoo, 1966). It is an annual winter herb, and the height of the plant is around three feet, with has open thin stem branches with pale yellow flowers (Ray *et al.*, 2005). The aerial parts of the plant are being used in traditional medicine to treat cough, rheumatism, inflammation, chest congestion, swelling and cleaning wounds (Lev, 2003). The seeds of the plant are used as an expectorant and in treating voice disorders (Shah *et al.*, 2014). Different studies revealed that the *S. irio*

species contain various metabolites such as alkaloids, steroids, flavonoids, anthraquinones and fatty acids (Al-Jaber, 2011; Al-Qudah and Abu Zarga, 2010 a; Vahora *et al.*, 1980). Many phytochemicals have been isolated through different studies from various parts of *S. irio* such as alkaloids, tannin, saponins, flavonoids, glycosides, phenolics, glucosinolates, carbohydrates, fatty acids, amino acids, proteins and steroids that contribute to various pharmacological actions such as antibacterial, antifungal, anti-inflammatory, anticancer, analgesic, antipyretic, hepato-protective and broncho-protective (Hailu *et al.*, 2019). Studies showed that the aerial parts of *S. irio* exhibit significant antibacterial activities against gram-positive and negative bacterial strains (Shabnam *et al.*, 2015; Al-Massarani *et al.*, 2017). Hence, with the aim to identify the probable site of action of natural antibacterial compounds in conjunction with their efficacy, the extracted phytochemicals from different parts of *S. irio*, have been used as a screening dataset against a well know bacterial drug target. Molecular docking is a widely used technique to help researchers to predict the arrangement of small molecules within the 3D structure of the receptor along with the affinity of the ligand to the target with appreciable accuracy and efficacy (Kroemer, 2007 and Kumalo *et al.*, 2015). The availability of protein molecule's three-dimensional (3D) structure and high-end computation facilities has made it more feasible than ever before. The well-known antibacterial drug target used in the present study is DHFR, isolated from *Staphylococcus aureus*, PDB ID: 3SRW. DHFR is an essential enzyme, involved in catalysing the transfer of a hydride ion (H<sup>-</sup>) from nicotinamide adenine dinucleotide phosphate (NADPH) to 7,8 dihydrofolate (DHF), results in forming 5,6,7,8 tetrahydrofolate (THF) as a product. It is the principle enzymes of THF pathway, involved in maintain the pools of THF and its derivatives inside the cell. THF and its derivatives act as an essential cofactors in many single-carbon transfer reactions such as biosynthesis of purine nucleotides, thymidylate, panthothenate and other metabolites. Inhibition of DHFR blocks DNA replication and cell division, resulting in cell death (Oefner *et al.*, 2009). The amino-acid residues present in the active site of DHFR are as follows Asp<sup>28</sup>, Leu<sup>29</sup>, Val<sup>32</sup>, Leu<sup>55</sup>, Ile<sup>57</sup> and Phe<sup>93</sup>. DHFR is also a famous target enzyme against antibacterial, antifungal, antiparasitic and anticancerous agents and Trimethoprim is one of the most popularly used antibiotic against it. However, with the advent of time, both gram-positive and gram-negative bacteria have developed resistance against trimethoprim (Li *et al.*, 2011). Therefore, there is an urgent need to search for suitable replacements for this conventionally used antibiotic with maximum efficacy and minimal side effect.

Techniques like molecular docking and virtual screening are routinely used to unveil the binding potential for

respective conformations of small molecules against the receptor. However, the freely available tools like: AutoDock4 and AutoDock Vina used for molecular docking fails to segregate the false positive and negative controls, hence, post-processing by the incorporation of MD simulation of the docked complexes is always advised for accurate docked orientation and ranking the top hits based on estimated binding free energies ( $\Delta G_{\text{bind}}$ ) (Gupta *et al.*, 2018). Among the various popular methods, molecular mechanics Poisson-Boltzmann surface area (MMPBSA) and molecular mechanics generalized born surface area (MMGBSA) are widely used for predicting binding affinities of receptor-ligand complexes (Massova and Kollman, 2000), as the above two techniques favours well-converged systems of receptor-ligand complexes generated during molecular dynamics (MD) simulation. Therefore, 'Gromacs' an open-source MD simulation package has been deployed to generate equilibrated trajectories of water-soaked receptor-ligand complexes (Pronk *et al.*, 2013). On the above simulated well-stabilized trajectories, binding free energy calculation was performed using 'g\_mmpbsa' tool to estimate the affinity between receptor (DHFR) and phytochemicals. The availability of 3D-structure renders feasibility to the SBDD (Structure-based drug designing) approach to discover novel antimicrobial compounds.

The present study aimed to identify potential candidates against antibacterial drug target, i.e. *S. aureus* DHFR (saDHFR), using nature derived phytochemicals from *S. irio*. Virtual screening and molecular dynamics simulation (using gromacs) were performed to estimate the binding affinity of *S. irio* derived phytochemicals against *S. aureus* DHFR.

## MATERIALS AND METHODS

### Library preparation

Over a few decades, molecular docking has gained rapid acceleration in the field of computational drug discovery. It involves the estimation of binding poses and energies corresponding to the generated conformations. The phytochemicals identified from the aerial parts of *S. irio* were used to prepare virtual library and screened against well-known antibacterial drug target DHFR from *S. aureus* (PDB ID: 3SRW). Total 79 compounds (phytochemicals) identified in different studies (Khan *et al.*, 1991; Griffiths *et al.*, 2001; Al-Qudah and Abu Zarga, 2010 a and b; Al-Jaber, 2011; Alsaffar *et al.*, 2016 and Al-Massarani *et al.*, 2017) were used as an initial dataset. The smile structures of all the compounds were copied from the Pubchem database (Kim *et al.*, 2016) and pasted on Molinspiration software to find out their drug likeness. Finally, 29 phytochemicals were filtered through Molinspiration software and found to follow all the rules of lipsinki rule of five and thus se-

lected for further analysis. Table 1 summarizes the list of 29 phytochemicals with Pubchem CID, along with the acceptable molecular weight values, no hydrogen bonds acceptor (nON), no Hydrogen bonds donor (nOHNH) and partition coefficient, required for a compound to act as drug. The compounds were downloaded in 3D sdf format and further converted to mol2 using Open Babel tool (O'Boyle *et al.*, 2011). The well-known drug against bacterial DHFR i.e. Trimethoprim was taken as a positive control. Further, an inbuilt script 'prepare\_ligand.py' of MGL Tool was used for batch conversion of ligands from mol2 format to Autodock Vina's compatible format (pdbqt) to perform virtual screening (Morris *et al.*, 2009; Trot and Olson, 2010).

### Receptor preparation

The 3-dimensional crystal structure of DHFR (PDB-ID 3SRW) was downloaded from RCSB database. 3SRW is a co-crystal structure with NADPH and a ligand bound at active sites. NADPH was kept intact throughout the screening. For molecular docking using AutodockVina, the receptor too needs to be present in pdbqt format, which was achieved using 'prepare\_receptor.py' script incorporated in MGL Tools (Morris *et al.*, 2009).

### Molecular docking

As, the PDB-3SRW is a co-crystal structure, its active site is well characterised, yet to get the coordinates (grid centre; x,y,z) lying in the active site for molecular docking, Putative Active Site with Spheres (PASS) package was employed that characterized regions of buried volume to identify binding sites based on shape, size and burial extent of volumes (Brady and Stouten, 2000). The molecular docking was performed using Autodock Vina software with the grid size of x, y, z=25 and run number of 10. Pymol was used to visualise the bound confirmation of small molecules to the receptors (DeLano, 2002). The interactions of the docked receptor-ligand complexes (H-bond & hydrophobic interactions) were analysed using Ligplot+ program (Laskowski and Swindells, 2011). Out of multiple conformations generated by AutoDock Vina, the one with the least energy was selected for post-processing.

### Molecular dynamics simulations

An all-atom MD simulation was performed on the receptor-small-molecules (Trimethoprim, CID\_5280443 and CID\_5280863) complexes using GROMACS 5.5.1 (<http://www.gromacs.org/>) via TIP3P water model (Van Der Spoel *et al.*, 2005). The 'pdb2gmx' program was used to allocate missing force-field parameters to the receptor that parameterised using ff99SB-ILDN force-field (Lindorff-Larsen *et al.*, 2010). The molecular mechanics parameters of all three ligands and NADPH molecule have been assigned using the 'antechamber'

module of AMBER18 using the AM1-BCC charge method (Jakalian *et al.*, 2002), and generalized amber force-field (gaff) (Wang *et al.*, 2004). The AMBER parameter database was used to obtain the parameters for NADPH (<http://research.bmh.manchester.ac.uk/bryce/amber/>) and further converted to Gromacs compatible format using a python script 'Acpype.py' (Sousa da silva and Vranken, 2012). After that, the receptor-ligand complex was immersed in a 1.0 nm thick cubic box. The 'editconf' tool was used to apply PBC conditions by the addition of SPC water molecules to all the three systems. Since, all three ligands possess zero net charge, the 'genion' tool added 9 Na<sup>+</sup> ions to neutralize the three different systems successfully. It was first energy minimized, to remove the bad contacts from the above systems, followed by a short NVT simulation (100 ps at 300K temperature). Subsequently, another 100 ps of simulation, at NPT ensemble (atmospheric pressure; 1 bar) along with position restraints on the macromolecule was performed to equilibrate the system. Once ensured that the systems were well equilibrated, they were subjected to a final production run for 100 ns, with time-step (2 fs). The 'Parrinello-Rahman' and 'V-rescale' thermostat algorithm was deployed as pressure and temperature coupling methods. During production phase, a number of vital parameters such as root-mean-square deviation (RMSD), root-mean square fluctuation (RMSF), radius of gyration (Rg) and solvent accessible surface area (SASA) were calculated from the trajectory (written every 10 ps) to investigate the dynamic stability of the receptor-ligand complexes. The principal component analysis (PCA) or essential dynamics (ED) of the MD trajectories was also performed to lessen the complication of the MD simulation coordinates to recognize the most significant motions. The eigenvalues and eigenvectors attained by diagonalizing the covariance matrix and the carbon-alpha motions of the two principal components (PC1 and PC2) were further inspected by the ED method. The 'Qtgrace', a plotting tool, generates all the graphs (<https://sourceforge.net/projects/qtgrace/>). The binding efficacy of each compound towards the DHFR receptor was assessed by the computation of binding free energy ( $\Delta G_{\text{bind}}$ ) via MMPBSA approach with the help of the g\_mmpbsa tool (Kumari *et al.*, 2014).

### Binding free energy estimation

Incorporated with MD simulation, binding free-energy calculation methods have emerged as robust mechanisms in bestowing quantifiable estimation for protein-protein and protein-ligand interactions. It is a crucial tool to explore the dynamic nature of the ligand inside the receptor cavity. A Gromacs compatible tool, 'g\_mmpbsa' was used to compute the binding free energy ( $\Delta G_{\text{bind}}$ ) between the receptor (DHFR enzyme) and the ligand of well equilibrated complex trajectories.

Here, all the energy components were calculated on 70 to 100 ns data at the time interval of 500 ps.

## RESULTS AND DISCUSSION

Current research work is focused on predicting the inhibitory potential of the phytochemicals derived from aerial parts of *S. irio* against saDHFR enzyme. In the present study *in-silico* technique such as molecular docking was performed to predict the binding affinity and conformations of the small molecules to the above receptor. Detailed molecular docking analysis of the interactions between the receptor and the ligands has given some valuable compounds possessing the lowest binding scores compared to the positive control, which formed the base for selecting the top hits. Later, the behaviour of top molecules and positive control are studied in a dynamic state using the molecular dynamics approach.

### Molecular docking analysis

Molecular docking is a widely used computational method to predict the mode of binding of chemical compounds to any specific receptor. The docking score and the molecules' conformation decide the compounds' affinity against the receptor. Fig.1 shows the binding conformations of the top five ligands in the active site pocket of the DHFR receptor. The NADPH molecule is bound at the site adjacent to the active site. Table 2 represents the top five compounds and the positive controls docked to DHFR receptor along with their AutoDock Vina score and residues interacting with the compounds. Compound CID\_5280443, CID\_5280863 and CID\_5280343 had the docking score of -8.5, -8 and -7.9 kcal/mol respectively. These three compounds possess docking score even better than the positive control trimethoprim (-7.0 kcal/mol), though they possess lesser number of H-bonds. Compound CID\_5280443 and CID\_5280863 form 2 H-bond along with 8 and 6 lipophilic interactions, whereas CID\_5280343 forms 1 H-bond and 7 lipophilic interactions. It has been observed here that more hydrophobic interactions correspond to lower binding score hence, strong affinity towards the receptor. Therefore, out of 29 phytochemicals, the compounds that exhibited lower binding scores than the trimethoprim, in conjunction with the conformational stability offered by the interactions among the receptor and the ligand via LigPlot+, laid the basis for selecting the top hits. The selected top hits and the positive control are subsequently promoted to MD simulation to estimate their conformational stability and the binding strength with the receptor.

### Molecular dynamics simulations

Molecular dynamics simulation analysis has served as an excellent approach to understanding the behaviour

of receptor and ligand with respect to each other in bound form. Here, we performed the explicit receptor-ligand complex simulations to evaluate the stabilities of the small-molecules at the binding pocket of the receptor protein using the root mean square deviation (RMSD), root mean square fluctuation (RMSF), radius of gyration (Rg), hydrogen bond (H-bond), solvent accessible surface area (SASA), principal component analysis (PCA) and binding free energy ( $\Delta G_{\text{bind}}$ ) computation using 'g\_mmpbsa tool'.

The RMSD analysis is used to access the conformational stability of the receptor and small-molecule in bound complex form during the MD run. Technically, the RMSD computes the deviations in the protein backbone from the initial to the final conformation, stating that lesser deviations correspond to a more stable protein (Aier et al., 2016). In the present study, the RMSD analysis was performed for the protein receptor backbone (REC-BB), receptor-ligand complex (REC-LIG-COM), receptor-ligand-NADPH complex (REC-LIG-NADPH-COM) and only ligands for both the compounds as well as for trimethoprim. Fig. 2A, 2B, 2C and 2D represent the REC-BB (black), REC-LIG-COM (red) and REC-LIG-NADPH-COM (green) RMSD plot for trimethoprim, compound CID\_5280443 and CID\_5280863 respectively over 100 ns data. All three RMSD plots of trimethoprim overlap and converge around 70 ns to the deviation of ~0.1 nm. This suggests that the trimethoprim exhibits stability at the active site vicinity of the receptor and forms an established complex in the presence of NADPH. The REC-LIG-COM and REC-LIG-NADPH-COM graphs for compounds CID\_5280443 and CID\_5280863 are almost overlapping. However, a surge is observed for the REC-LIG-COM RMSD profile of CID\_5280443 and CID\_5280863 that further settles around 60 ns, indicating that the docked conformation was not appropriate initially, but it eventually stabilizes at the binding site. Furthermore, compound CID\_5280443 in complex form exhibits a little higher RMSD (0.2 nm) as compared to the backbone (0.1 nm), but both the plots demonstrate stable RMSD profile from 60 to 100 ns, whereas the RMSD profile of CID\_5280863 remained steady for both the REC-BB (black) and REC-LIG-COM (red) (0.1 nm). Moreover, the RMSD profile only for ligands shows a well-converged graph for trimethoprim (around 0.5 nm), and CID\_5280863 however, CID\_5280443 exhibits a bit higher deviation from 0.5 nm to ~1.0 nm. Also, none of the ligands exhibits more than 0.1 nm deviation in their RMSD profile. The above analysis suggests that the concerned ligand remained stable in the binding pocket of the receptor. Therefore, it can be inferred that MD simulation studies up-scales the results of any docking process that allows the small molecules to properly align into the binding cavity of the receptors, in a manner that promotes stabilized energy conformation.

**Table 1.** List of phytochemicals from *S. irio* aerial parts, following the Lipinski rule of five

Phytochemicals	PubChem CID	Molecular weight	nON	nOHNH	mi LogP	References
Quercetin	5280343	302.24	7	5	1.68	Khan <i>et al.</i> , 1991
Isorhamanetin	5281654	316.26	7	4	1.99	Khan <i>et al.</i> , 1991
N-(n-propyl) acetamide	21407	101.15	2	1	0.34	Al-Qudah and Abu Zarga, 2010 b
Isopropyl isothiocyanate	75263	101.17	1	0	2.28	Al-Qudah and Abu Zarga, 2010 b
Isobutyl isothiocyanate	68960	115.20	1	0	2.73	Al-Qudah and Abu Zarga, 2010 b
n-butyl isothiocyanate	11613	115.20	1	0	3.04	Al-Qudah and Abu Zarga, 2010 b
Indole-3-carboxaldehyde	10256	145.16	2	1	1.88	Al-Qudah and Abu Zarga, 2010 a
Indole-3-carboxylic acid	69867	161.16	3	2	1.66	Al-Qudah and Abu Zarga, 2010 a
Apigenin	5280443	270.24	5	3	2.46	Al-Jaber, 2011
Adenosine	60961	267.25	9	5	-0.85	Al-Qudah and Abu Zarga, 2010 a
Kaempferol	5280863	286.24	6	4	2.17	Al-Jaber, 2011
Nicotine	89594	162.24	2	0	1.09	Alsaffar <i>et al.</i> , 2016
2E-Hexenal	10464307	98.14	1	0	2.33	Al-Qudah and Abu Zarga, 2010 b
Dimethyl sulphone	6213	94.14	2	0	-0.29	Al-Qudah and Abu Zarga, 2010 b
beta-Terpinyl acetate	88693	196.29	2	0	3.32	Al-Qudah and Abu Zarga, 2010 b
Nonanal	31289	142.24	1	0	4.10	Al-Qudah and Abu Zarga, 2010 b
trans-z- $\alpha$ -Bisabolene epoxide	91753504	220.36	1	0	4.64	Al-Qudah and Abu Zarga, 2010 b
p-Anisaldehyde	31244	136.15	2	0	1.78	Al-Qudah and Abu Zarga, 2010 b
Indole	798	117.15	1	1	2.16	Al-Qudah and Abu Zarga, 2010 b
p-Vinylguaiaicol	332	150.18	2	1	2.13	Al-Qudah and Abu Zarga, 2010 b
1,5,8-Trimethyl-1,2-dihydronaphthalene	137331947	172.27	0	0	3.87	Al-Qudah and Abu Zarga 2010 b
1,1,6-Trimethyl-1,2-dihydronaphthalene	121677	172.27	0	0	4.14	Al-Qudah and Abu Zarga, 2010 b
1,1,6-Trimethyl-1,2,3,4-tetrahydronaphthalene	68057	174.29	0	0	4.29	Al-Qudah and Abu Zarga, 2010 b
o-Benzyl-L-serine	78457	195.22	4	3	-1.46	Al-Qudah and Abu Zarga, 2010 b
3-Methyl indole	6736	131.18	1	1	2.54	Al-Qudah and Abu Zarga, 2010 b
Isovanillin	12127	152.15	3	1	1.07	Al-Qudah and Abu Zarga, 2010 b
4-(2,4,4-trimethyl-cyclohexa-1,5-dienyl) but-3-en-2-one	5363898	190.29	1	0	3.19	Al-Qudah and Abu Zarga, 2010 b
Methoxyeugenol	226486	194.23	3	1	2.12	Al-Qudah and Abu Zarga, 2010 b
2-(2-Methylpropylidene)-1H-indene-1,3(2H)-Dione	608287	200.24	2	0	2.42	Al-Qudah and Abu Zarga, 2010 b

\*nON= no of Hydrogen bonds acceptor, nOHNH= no of Hydrogen bonds donor

The extent to form polar interactions between small molecules and receptor was investigated by identifying the number of hydrogen bonds (H-bonds) between the receptor and ligand during the simulation Fig.3. From the plot, it can be inferred that the trimethoprim possess maximum number of H-bonds with the receptor throughout the 100 ns simulation, whereas

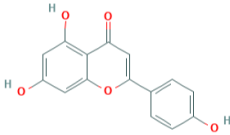
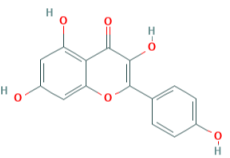
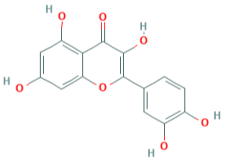
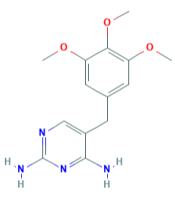
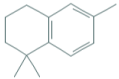
CID\_5280863 and CID\_5280443 forms a significant number of H-bond interactions however, higher occupancy is observed for the former one. Thus, the above results suggest that the aforementioned phytochemicals can be considered as a promising candidate against *S. aureus* DHFR enzyme.

The RMSF was monitored throughout the simulation to

understand the fluctuation of each amino acid during the MD run. The RMSF profile of the protein for the three independent systems: trimethoprim (black), CID\_5280863 (red) and CID\_5280443 (green) are shown in Fig. 4A. As observed from the RMSF plots,

higher fluctuations are observed for following amino acids <sup>67</sup>TSFNVE<sup>72</sup>, F119, F129, K141 and E144 for all the three systems. Furthermore, mapping the aforementioned amino acids on the structure file revealed that these amino acids are primarily part of the loops

**Table 2.** Top five compounds and the positive controls docked to DHFR receptor along with their AutoDock Vina score, number of interactions and residues interacting with the compounds

Compound ID	Structure	Autodock Vina score (kcal/mol)	Number of H-bonds and residues involved	Number of lipophilic interactions and residues involved
CID_5280443		-8.5	2; Gln20, Asp28	8; Leu6, Val7, Ala8, Leu21, Leu29, Ser50, Ile51, Phe93
CID_5280863		-8	2; Gln20, Asp28	6; Val7, Leu21, Leu29, Ser50, Ile51, Phe93
CID_5280343		-7.9	1; Gln20	7; Leu6, Val7, Ala8, Leu21, Asp28, Ser50, Ile51, Phe93
CID_5578 Trimethoprim		-7	3; Leu6, Asp28, Phe93	5; Val7, Ala8, Leu21, Leu29, Val32
CID_68057		-7	-	8; Leu21, Asp28, Leu29, Val32, Thr47, Ile51, Leu55, Phe93

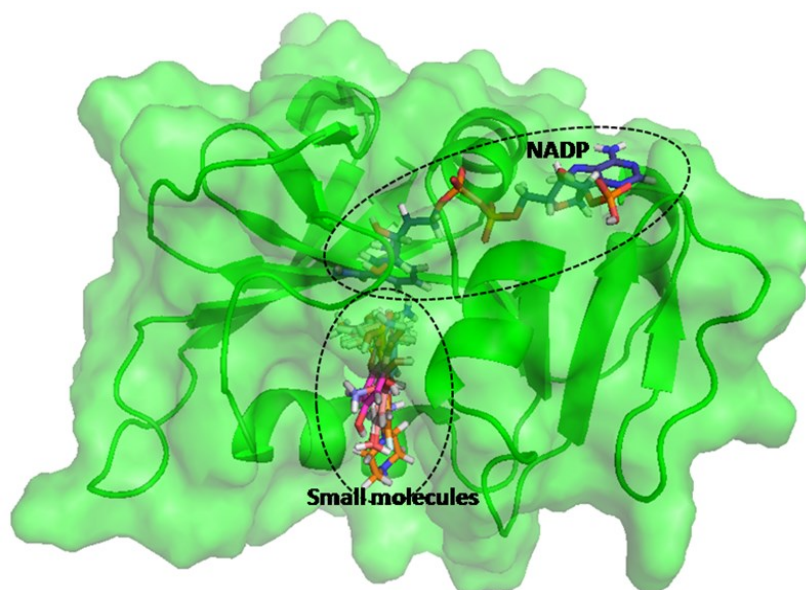


**Fig.1.** Binding conformations of the top five ligands in the active site pocket of the DHFR receptor

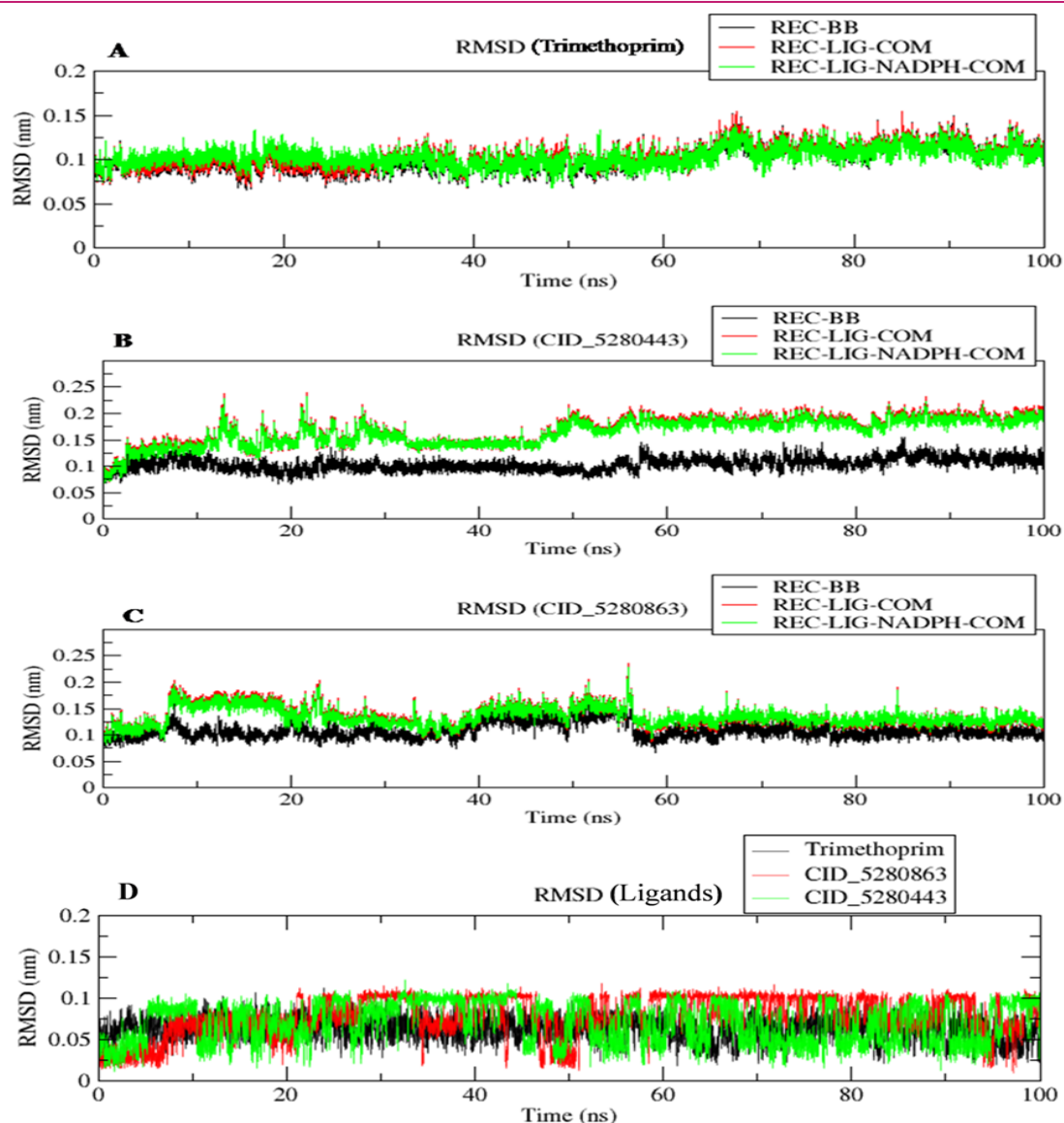


**Fig. 2.** RMSD profiles of (A) Trimethoprim (B) CID\_5280443 and (C) CID\_5280863 for receptor-backbone/REC\_BB (black), receptor-ligand-complex/REC-LIG/COM (red) and receptor-ligand-NADPH-complex/REC-LIG-NADPH-COM (green) respectively

**Table 3.** Individual energy components and their contributions to the binding free energy ( $\Delta G_{\text{bind}}$ ) for both the phytochemicals and the positive control

Compound	van der Waal energy (kJ/mol $\pm$ Std.dev)	Electrostatic energy (kJ/mol $\pm$ Std.dev)	Polar solvation energy (kJ/mol $\pm$ Std.dev)	SASA energy (kJ/mol $\pm$ Std.dev)	Binding energy; $\Delta G_{\text{bind}}$ (kJ/mol $\pm$ Std.dev)
Trimethoprim (positive control)	-101.256 $\pm$ 1.104	-15.962 $\pm$ 1.196	72.963 $\pm$ 1.252	-16.578 $\pm$ 0.096	-60.609 $\pm$ 1.221
CID_5280443	-98.451 $\pm$ 1.421	-22.734 $\pm$ 1.166	63.979 $\pm$ 1.826	-12.125 $\pm$ 0.133	-69.209 $\pm$ 1.478
CID_5280863	-114.634 $\pm$ 1.168	-13.604 $\pm$ 1.340	66.584 $\pm$ 1.651	-13.103 $\pm$ 0.124	-74.928 $\pm$ 1.517

and reside way off from the active site; hence, little higher fluctuations will not influence the binding of small-molecule to the receptor. These results infer that the presence of compounds has not caused any major fluctuation in amino acid residues of the enzyme during the simulation.

Rg is a measure of the compactness of the protein (Lobanov *et al.*, 2008). Fig.4B depicts the measured Rg for the backbone atoms for all three systems trimethoprim (black), CID\_5280863 (red) and CID\_5280443 (green). The Rg plots for the above systems remained steady throughout the simulation run, representing the

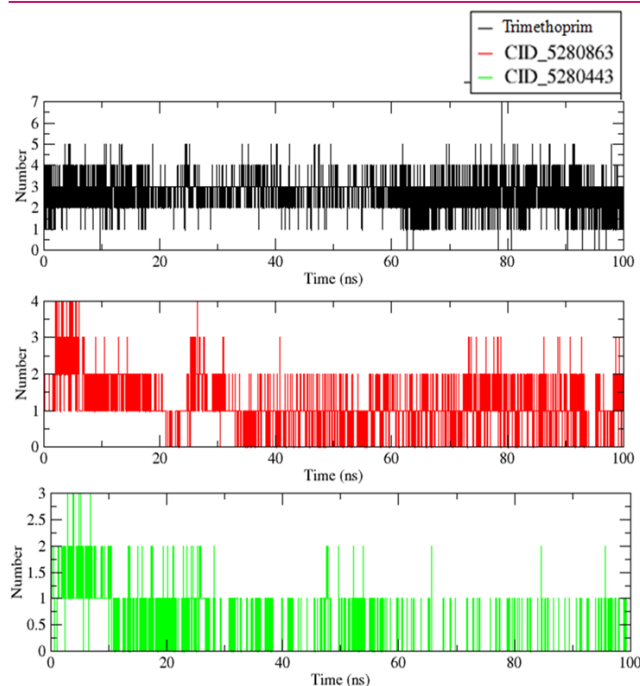


**Fig.3.** Number of H-bonds identified during the 100 ns simulation for trimethoprim (black), CID\_5280863 (red) and CID\_5280443 (green)

high compactness of the protein in all three systems portraying that the compounds did not hamper the native structure of the enzyme. The SASA value (Fig.4C) is in the range of  $\sim 93\text{nm}^2$  for all three systems, deciphering the presence of phytochemicals (CID\_5280863 and CID\_5280443) in the active site cavity of the receptor does not allocate any major structural change in the receptor's geometry. The above analysis confirms that the trimethoprim and the phytochemicals do not perturb the configuration of the enzyme and the stability is conserved close to its native form. Overall, the RMSD profile of all three molecules (CID\_5280443, CID\_5280863 and trimethoprim) exhibits stability around 70 ns. Hence initial 70 ns data will not be considered for binding free energy estimation.

The essential subset gives the maximum protein dynamics that can be recognised with eigenvectors which are mostly associated with the eigenvalues. The dynamic behaviour of the DHFR receptor in the presence of trimethoprim (Fig.5A.) and the proposed phytochemicals (CID\_5280863 and CID\_5280443) (Fig.5B & 5C) is illustrated in the form of PC1 vs. PC2 2D projection plots. The results revealed that the clusters representing the C $\alpha$ -atoms of the receptor from three different

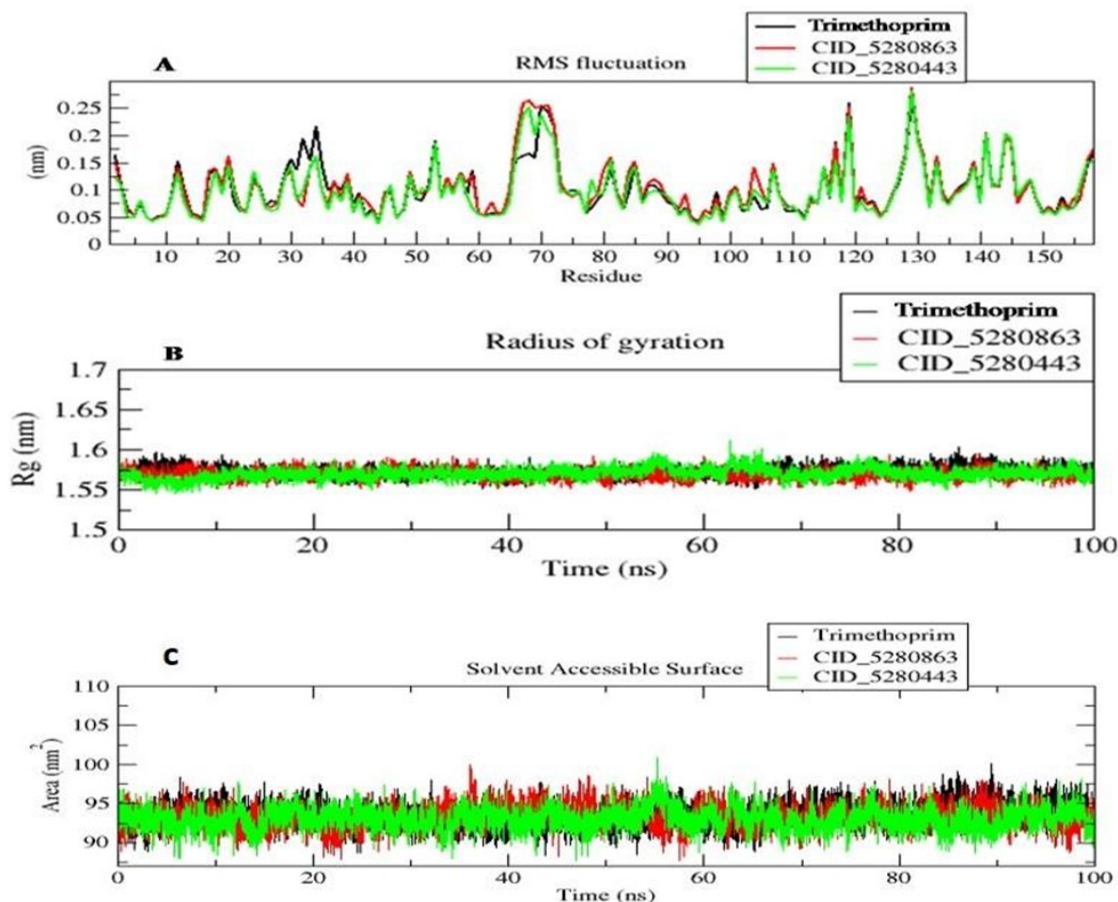


**Fig. 4.**(A) RMS fluctuation profiles and (B) The radius of gyration and (C) Solvent accessible surface area (SASA) of trimethoprim (black), CID\_5280863 (red) and CID\_5280443 (green) bound enzyme respectively

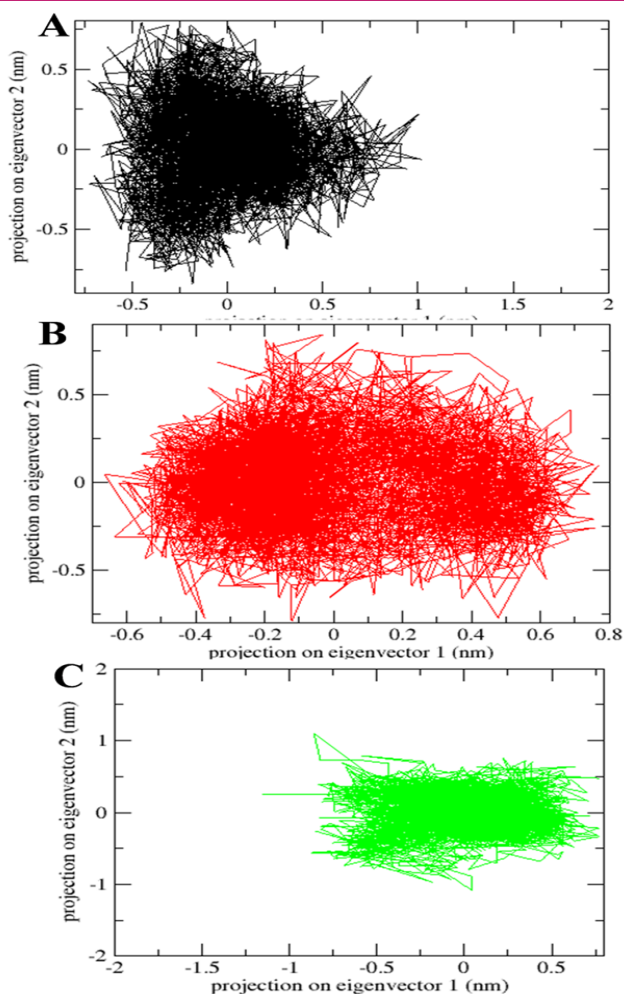


**Fig. 5.** PCA results of (A) Trimethoprim (black), (B) CID\_5280863 (red) and (C) CID\_5280443 (green) showing plot of PC2 vs PC1

systems are well-defined by covering the minimum regions. However, the differences in the cluster size and PCs rearrangements were majorly due to the change in the structure of the ligands. Therefore, ligand binding does not generate any novel motions in the structure, but rather rearranges motions energetically in the dynamic range of the structure.

### Binding free energy estimation

Additionally, to estimate the strength of binding of the above compounds to the receptor, g\_mmpbsa tool has been deployed. The  $\Delta G_{\text{bind}}$  and the contribution of individual components for both the ligands and the positive control are tabulated in Table 3. The  $\Delta G_{\text{bind}} = \text{kJ/mol}$  for -69.209 CID\_5280443, -74.928 kJ/mol for CID\_5280863 and -60.609 kJ/mol for trimethoprim, respectively.

*S. aureus* and other bacterial infections are the primary concern to public health due to the development of resistance against antibiotics. Many efforts have been made to develop a suitable replacement for commer-

cially used antibiotics against *S. aureus*. One such study by Bourne *et al.* (2010) where a small molecule RAB1 (co-crystal *Bacillus anthracis* DHFR inhibitor) was found to be effective in binding the saDHFR as well. In another independent study, a three-step screening was performed on the saDHFR crystal structure using a chemical compound library. This study revealed five compounds (KBS1-KBS5) based on docking and simulations results, out of which, three compounds (KBS1, KBS3 and KBS4) exhibited *in-vitro* efficacy against wild-type as well as mutated saDHFR (Kobayashi *et al.*, 2014). A recent *in-silico* study revealed two lead molecules exhibiting higher affinity towards saDHFR validated via MMGBSA method (Singh *et al.*, 2022). Understandably, various efforts have been underway to find alternative antibiotics against *S. aureus*, but significantly less contribute to medicinal plant products.

Although many studies have already been done on the antimicrobial activities from aerial parts of *S. irio* against both gram-positive and gram-negative bacteria (Shabnam *et al.*, 2015; Al-Massarani *et al.*, 2017; El-Sherbiny *et al.*; 2017), but none of the studies were done for the exploration of most potential phytochemical from *S. irio* responsible for the antibacterial property and its mechanism of antibacterial action. Therefore, the present research deciphers the virtual-screening of 29 selected phytochemicals from *S. irio* against saDHFR. The results confer that 3 phytochemicals show better Vina score with the receptor than the positive control (Trimethoprim). Out of three, the top two best-scored phytochemicals CID-5280863 (Kaempferol) and CID-5280443 (Apigenin) were further validated using MD simulation studies. The MD simulation studies have shown stable binding confirmations throughout the run. The affinity of both the phytochemicals for the DHFR receptor of *S. aureus* is higher than the positive control. The binding energies are also comparatively good compared to the most recent study (Singh *et al.*, 2022). Moreover, previous studies exhibit the presence of a high percentage of both flavonoids (Kaempferol and Apigenin) in the aerial parts of *S. irio* (Al-Jaber, 2011), which shows the importance of the plant as the source of antibacterial agents and also gives the scientific proof to the folkloric claim of the plant. The above results prove that the compounds are the suitable binder of the antibacterial drug target DHFR, and can act as the right candidate that can later be optimised to tackle the resistance against antibiotics.

### Conclusion

To address the problem of multi-drug resistance, a series of phytochemicals derived from the aerial parts of the plant *S. irio*, along with positive-control trime-

thoprim, screened against the active-site cleft of the DHFR receptor of *S. aureus* showed that phytochemicals CID\_5280443 and CID\_5280863 ranked at the top and exhibited lower docking scores compared to trimethoprim. The detailed analysis of their effect on the enzyme was studied using the MD simulation approach and its in-built analysis modules: RMSD, RMSF, H-bond, SASA, Rg and PCA. Both the investigated phytochemicals were found to have comparable RMSD profile, RMSF and Rg to the positive control however, the binding free energy values indicate a significant difference. Both phytochemicals also made a significant number of Hydrogen bonds with the receptor. These results showed that among various phytochemicals, CID\_5280863 and CID\_5280443 appeared to be strong binders which can further be optimized to attain potential therapeutics against *S. aureus* infections with minimal chance of side effects. Thus, it can be concluded that *S. irio* is a powerful candidate for discovering bioactive compounds possessing antimicrobial activities and may also serve for the development of novel pharmaceuticals.

## ACKNOWLEDGEMENTS

Authors thank their parent Institutions for their support and assistance during the work and scientific writing.

## Conflict of interest

The authors declare that they have no conflict of interest.

## REFERENCES

- Adwan, G., Abu-Shanab, B. & Adwan, K. (2010). Antibacterial activities of some plant extracts alone and in combination with different antimicrobials against multidrug-resistant *Pseudomonas aeruginosa* strains. *Asian Pacific Journal of Tropical Medicine*, 3(4), 266-269. [https://doi.org/10.1016/S1995-7645\(10\)60064-8](https://doi.org/10.1016/S1995-7645(10)60064-8).
- Aier, I., Varadwaj, P. & Raj, U. (2016). Structural insights into conformational stability of both wild-type and mutant EZH2 receptor. *Scientific Reports*, 6, 34984. <https://doi.org/10.1038/srep34984>.
- Al Akeel, R., Al-Sheikh, Y., Mateen, A., Syed, R., Janardhan, K. & Gupta, VC. (2014). Evaluation of antibacterial activity of crude protein extracts from seeds of six different medical plants against standard bacterial strains. *Saudi Journal of Biological Sciences*, 21(2), 147–151. doi: 10.1016/j.sjbs.2013.09.003
- Al-Jaber, NA. (2011). Phytochemical and biological studies of *Sisymbrium irio* L. Growing in Saudi Arabia. *Journal of Saudi Chemical Society*, 15(4), 345-350. <https://doi.org/10.1016/j.jscs.2011.04.010>
- Al-Massarani, SM., El Gamal, A.A., Alam, P., Al-Sheddi, E.S., Al-Oqail, M.M. & Farshori, N.N. (2017). Isolation, biological evaluation and validated HPTLC-quantification of the marker constituent of the edible Saudi plant *Sisymbrium irio* L. *Saudi Pharmaceutical Journal*, 25(5), 750-759. <https://doi.org/10.1016/j.jpsp.2016.10.012>
- Al-Qudah, M.A. & Abu Zarga, M.H. (2010 a). Chemical constituents of *Sisymbrium irio* L. from Jordan. *Natural Product Research*, 24(5), 448-456. <https://doi.org/10.1080/14786410903388025>
- Al-Qudah, M.A. & Abu Zarga, M.H. (2010 b). Chemical composition of essential oils from aerial parts of *Sisymbrium irio* from Jordan. *Journal of Chemistry*, 7, 6-10. <https://doi.org/10.1155/2010/973086>
- Alsaffar, D.F., Abbas, I.S. & Dawood, A.H. (2016). Investigation of the Main Alkaloid of London Rocket (*Sisymbrium irio* L) as a Wild Medicinal Plant Grown in Iraq. *International Journal of Pharmaceutical Sciences Review and Research*, 39, 279-281.
- Alves, M.J., Froufe, H.J.C., Costa, A.F.T., Santos, A.F., Oliveira, L.G. & Osorio, S.R.M. (2014). Docking Studies in Target Proteins Involved in Antibacterial Action Mechanisms: Extending the Knowledge on Standard Antibiotics to Antimicrobial Mushroom Compounds. *Molecules*, 19(2), 1672-1678. <https://doi.org/10.3390/molecules19021672>.
- Bourne, C.R., Barrow, E.W., Bunce, R.A., Bourne, P.C., Berlin, K.D. & Barrow, W.W. (2010). Inhibition of antibiotic-resistant *Staphylococcus aureus* by the broad-spectrum dihydrofolate reductase inhibitor RAB1. *Antimicrobial agents and chemotherapy*, 54(9), 3825-3833. <https://doi.org/10.1128/AAC.00361-10>.
- Brady, G. P. & Stouten, P. F. (2000). Fast prediction and visualization of protein binding pockets with PASS. *Journal of Computer-Aided Molecular Design*, 14(4), 383–401. DOI: 10.1023/a: 1008124202956
- DeLano, W. L. (2002). Pymol: An open-source molecular graphics tool. *CCP4 Newsletter on protein crystallography*, 40, 82-92.
- El-Sherbiny, Gamal M., Moghannem, S. A. & Sharaf, M. H. (2017). Antimicrobial activities and cytotoxicity of *Sisymbrium irio* L extract against multi-drug resistant bacteria (MDRB) and *Candida albicans*. *International Journal of Current Microbiology and Applied Sciences*, 6, 1-13. <https://doi.org/10.20546/ijcmas.2017.604.001>
- Gupta, S., Lynn, A. M. & Gupta, V. (2018). Standardization of virtual-screening and post-processing protocols relevant to in-silico drug discovery. 3 *Biotech*, 8(12), 1-7. <https://doi.org/10.1007/s13205-018-1523-5>
- Griffiths, D.W., Deighton, N., Birch, A.N., Patrian, B., Baur, R. & Städler, E. (2001). Identification of glucosinolates on the leaf surface of plants from the Cruciferae and other closely related species. *Phytochemistry*, 57(5), 693-700. [https://doi.org/10.1016/S0031-9422\(01\)00138-8](https://doi.org/10.1016/S0031-9422(01)00138-8)
- Hailu, T., Gupta, R.K. & Rani, A. (2019). *Sisymbrium irio* L.: A Herb used in the Unani system of medicine for broad spectrum therapeutical applications. *Indian Journal of Traditional Knowledge*, 18(1), 140-143. <http://nopr.niscair.res.in/handle/123456789/45672>.
- Jakalian, A., Jack, D. B. & Bayly, C. I. (2002). Fast, efficient generation of high-quality atomic charges. AM1-BCC model: II. Parameterization and validation. *Journal of Computational Chemistry*, 23(16), 1623-1641. DOI: 10.1002/jcc.10128
- Khan, M.S., Javed, K. & Hasnain Khan, M. (1991). Chemical constituents of the aerial parts of *Sisymbrium irio*. *Journal of the Indian Chemical Society*, 68, 532 DOI: 10.5281/

- zenodo.6155010
19. Khoshoo, T.N. (1966). Biosystematics of *Sisymbrium* Complex XII: Distributional pattern. *Caryologia*, 19(2), 143-150. <https://doi.org/10.1080/00087114.1966.10796212>
  20. Kim, S., Thiessen, P.A., Bolton, E., Chen, J., Fu, G., Gindulyte, A., Bryant, S. H. et al. (2016). PubChem substance and compound databases. *Nucleic acids research*, 44 (D1), D1202-D1213.
  21. Kobayashi, M., Kinjo, T., Koseki, Y., Bourne, C.R., Barrow, W.W. & Aoki, S. (2014). Identification of novel potential antibiotics against *Staphylococcus* using structure-based drug screening targeting dihydrofolate reductase. *Journal of Chemical Information and Modeling*, 54 (4), 1242-1253. <https://doi.org/10.1021/ci400686d>.
  22. Kroemer, R.T. (2007). Structure-Based Drug Design: Docking and Scoring. *Current Protein Peptide Science*, 8 (4), 312-328. <https://doi.org/10.2174/138920307781369382>
  23. Kumalo, H. M., Bhakat, S. & Soliman, M.E.S. (2015). Theory and applications of covalent docking in drug discovery: Merits and pitfalls. *Molecules*, 20, 1984-2000. <http://dx.doi.org/10.3390/molecules20021984>.
  24. Laskowski, R. A. & Swindells, M. B. (2011). LigPlotb: Multiple ligand-protein interaction diagrams for drug discovery. *Journal of Chemical Information and Modeling*, 51 (10), 2778-2786. DOI: 10.1021/ci200227u
  25. Lev, E. (2003). *Sisymbrium irio* medicinal Substances in Jerusalem from early times to the present day Archaeopress. Oxford, UK, p. 62.
  26. Li, X., Hilgers, M., Cunningham, M., Chen, Z., Trzoss, M., Zhang, J., Kohnen, L., Lam, T., Creighton, C., Kedar, G.C., Nelson, K. (2011). Structure-based design of new DHFR-based antibacterial agents: 7-aryl-2, 4-diaminoquinazolines. *Bioorganic Chemistry Letters Medicinal*, 21(18), 5171-5176. <https://doi.org/10.1016/j.bmcl.2011.07.059>.
  27. Lindorff-Larsen, K., Piana, S., Palmo, K., Maragakis, P., Klepeis, J. L., Dror, R. O. & Shaw, D. E. (2010). Improved side-chain torsion potentials for the Amber ff99SB protein force field. *Proteins: Structure, Function, and Bioinformatics*, 78(8), 1950-1958. DOI: 10.1002/prot.22711.
  28. Lobanov, M.Y., Bogatyreva, N.S. & Galzitskaya, O.V. (2008). Radius of gyration as an indicator of protein structure compactness. *Molecular Biology*, 42, 623-628. <https://doi.org/10.1134/S0026893308040195>
  29. Kumari, R. & Kumar, R., Open Source Drug Discovery Consortium & Lynn, A. (2014). g\_mmpbsa: A GROMACS tool for high-throughput MM-PBSA calculations. *Journal of Chemical Information and Modeling*, 54(7), 1951-1962. <https://doi.org/10.1021/ci500020m>.
  30. Massova, I. & Kollman, P. A. (2000). Combined molecular mechanical and continuum solvent approach (MM-PBSA/GBSA) to predict ligand binding. *Perspectives in Drug Discovery and Design*, 18(1), 113-135. <https://doi.org/10.1023/A:1008763014207>
  31. Morris, G. M., Huey, R., Lindstrom, W., Sanner, M. F., Belew, R. K., Goodsell, D. S. & Olson, A. J. (2009). AutoDock4 and AutoDockTools4: Automated docking with selective receptor flexibility. *Journal of Computational Chemistry*, 30(16), 2785-2791. DOI: 10.1002/jcc.21256
  32. O'Boyle, N. M., Banck, M., James, C. A., Morley, C., Vandermeersch, T. & Hutchison, G. R. (2011). Open Babel: An open chemical toolbox. *Journal of Cheminformatics*, 3, 33. <https://jcheminf.biomedcentral.com/articles/10.1186/1758-2946-3-33>.
  33. Oefner, C., Parisi, S., Schulz, H., Lociuo, S. & Dale, G.E. (2009). Inhibitory properties and X-ray crystallographic study of the binding of AR-101, AR-102 and iclaprim in ternary complexes with NADPH and dihydrofolate reductase from *Staphylococcus aureus*. *Acta Crystallographica Section D: Biological Crystallography*, 65(8), 751-757. <https://doi.org/10.1107/S0907444909013936>
  34. Pronk, S., Páll, S., Schulz, R., Larsson, P., Bjelkmar, P., Apostolov, R. & Lindahl, E. (2013). GROMACS 4.5: a high-throughput and highly parallel open source molecular simulation toolkit. *Bioinformatics*, 29(7), 845-854. DOI: 10.1093/bioinformatics/btt055
  35. Ray, J., Creamer, R., Schroeder, J. & Murray, L. (2005). Moisture and temperature requirements for London rocket (*Sisymbrium*) emergence. *Weed Science*, 53(2), 187-192. <https://doi.org/10.1614/WS-04-150R1>.
  36. Sousa da Silva, A. W. & Vranken, W. F. (2012). ACPYPE-Antechamber python parser interface. *BMC research notes*, 5(1), 1-8. <https://doi.org/10.1186/1756-0500-5-367>.
  37. Shabnam, B., Ziaur, R., Khalid, R. & Naveed, I. (2015). Biological screening of polarity-based extracts of leaves and seeds of *Sisymbrium* L. *Pakistan Journal of Botany*, 47, 301-305.
  38. Shah, S., Rehmanullah, S. & Muhammad, Z. (2014). Pharmacognostic standardization and pharmacological study of *Sisymbrium* L. *American Journal of Research Communication*, 1(7), 241-253.
  39. Singh, G., Soni, H., Tandon, S., Kumar, V., Babu, G., Gupta, V. & Chaudhuri, P. (2022). Identification of natural DHFR inhibitors in MRSA strains: Structure-based drug design study. *Results in Chemistry*, 26, 100292. <https://doi.org/10.1016/j.rechem.2022.100292>
  40. Trott, O. & Olson, A J. (2010). Software news and update AutodockVina: Improving the speed and accuracy of docking with a new scoring function, efficient optimization, and multithreading. *Journal of Computational Chemistry*, 31 (2), 455-461. doi: 10.1002/jcc.21334.
  41. Van Der Spoel, D., Lindahl, E., Hess, B., Groenhof, G., Mark, A. E. & Berendsen, H. J. C. (2005). GROMACS: Fast, flexible, and free. *Journal of Computational Chemistry*, 26(16), 1701-1718. <https://doi.org/10.1002/jcc.20291>.
  42. Vohora, S.B., Naqvi, S.A. & Kumar, I. (1980). Antipyretic, analgesic and antimicrobial studies on *Sisymbrium*. *Planta Medica*, 38(3), 255-259. DOI: 10.1055/s-2008-1074870.
  43. Wang, J., Wolf, R. M., Caldwell, J. W., Kollman, P. A. & Case, D. A. (2004). Development and testing of a general amber force field. *Journal of Computational Chemistry*, 25 (9), 1157-1174. DOI: 10.1002/jcc.20035.